

# Quantized Conductance

Valentina Watanabe

21367661

Lab partner: Ellen Lyons

October 2024

I have read and understood the plagiarism provisions in the General Regulations of the University Calendar for the current year, found at <http://www.tcd.ie/calendar>. I have also read and understood the guide, and completed the 'Ready Steady Write' Tutorial on avoiding plagiarism, located at <https://libguides.tcd.ie/academic-integrity/ready-steady-write>.

Signed: V.Watanabe Date: 04/10/24

## Contents

<b>1 Abstract</b>	<b>2</b>
<b>2 Introduction and Theory</b>	<b>2</b>
2.1 Density of States, 1D vs. 3D . . . . .	2
2.2 Conductance in Metal Wires . . . . .	4
2.3 Quantum Mechanical Model of a Nanowire . . . . .	5
2.4 Quantized Conductance . . . . .	7
<b>3 Experimental Method</b>	<b>9</b>
3.1 Analysing Simulated Data . . . . .	9
3.2 Acquiring and Analysing Experimental Data . . . . .	10
<b>4 Results and Discussion</b>	<b>11</b>
4.1 Simulated Data . . . . .	11
4.2 Gaussian Fitting on Simulation . . . . .	16
4.3 Experimental Data . . . . .	17
<b>5 Conclusion</b>	<b>20</b>
<b>6 References</b>	<b>21</b>

# 1 Abstract

The focus of this study is centred on the investigation of quantized conductance and its detection in nanowires. This is done by analyzing voltage transients associated with step changes in conductance. Simulations in ideal and non-ideal parameters are performed to then compare the yielding data taking into consideration the noise and uniformity. The data obtained in both ideal and non-ideal exhibits staircase patterns, with varying degrees of detail. Simulated data demonstrates peaks which should correspond to integer multiples of conductance quantum. Utilizing an oscilloscope, amplifier, and power source, we document the voltage transient and perform the same analysis as with the simulated data. As expected, the experimental data displays broader distributions lacking distinct peaks. This is because of noise and other factors that interrupt the recording of real-life quantum conductance in these circumstances. Despite these deviations, the research highlights the complexities of measuring quantum conductance in nanowires and proves that its presence can still be distinguished.

# 2 Introduction and Theory

The theory of quantized conductance arises from the principles of quantum mechanics, particularly in the context of electron transport through nanowires, such as one-dimensional (1D) conductors. It is relevant to explore how the quantization of conductance occurs as a result of discrete energy level formation in nanowires. This report details the relationship between the density of states and conductance, particularly highlighting the role of quantum mechanical behaviour in conductors. By analyzing both ideal and non-ideal scenarios, we aim to investigate how quantized conductance manifests in practical applications, providing insights into the underlying mechanisms of electron transport at the nanoscale.

## 2.1 Density of States, 1D vs. 3D

The density of the state of a material is a function that can be defined as the number of modes or states per unit energy range in one dimension. It describes the availability of the states at each energy level for the particles to occupy. It is also necessary to define the electron gas's total energy and thermal properties (Kittel, 2005). Its core equation is set to be

$$g_{1D} = \frac{1}{L} \frac{dN}{dE}. \quad (1)$$

The  $1/L$  represents the dimensionality (length) and  $dn/dE$  is the total number of states per unit energy. The approximation  $dn/dE$ , which is  $\approx \frac{\Delta n}{\Delta E}$ , improves as the length of the solid gets larger so that we start to observe an almost continuous energy distribution, with the discreteness from quantization becoming less pronounced (Kuno, 2012).

To derive a more instructive equation that incorporates geometry and quantum mechanics, we set it to a k-space and separate the definition with the chain rule.

$$g_{1D} = \frac{1}{L} \frac{dN}{dk} \frac{dk}{dE}. \quad (2)$$

Now let us consider a 1D structure, like a nanowire.

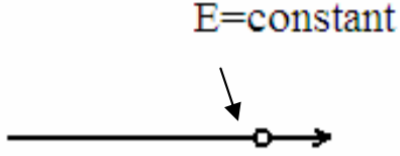


Figure 1: 1D structure (King, 2005).

We can write the k-space volume of a single-state cube and the k-space volume of a sphere as,

$$V_{single} = \frac{2\pi}{L} \quad (3)$$

and

$$V_{line} = kL. \quad (4)$$

To which we can then write the number of filled states in a sphere (5). We add a factor of two to account for the possible electron spins of the solution. We also add the correction factor to avoid the repetition of counting identical states (King, 2005).

$$N = \frac{V_{single}}{V_{line}} * 2 * \frac{1}{2} \quad (5)$$

$$N = \frac{2k}{\pi}. \quad (6)$$

Substituting  $k = \sqrt{\frac{2mE}{\hbar^2}}$  yields,

$$N = \frac{2}{\hbar\pi} \sqrt{2mE}. \quad (7)$$

Then, we differentiate.

$$\frac{dn}{dE} = \frac{dn}{dk} \frac{dk}{dE} = \frac{1}{2} \frac{2}{\hbar\pi} \sqrt{\frac{2m}{E}}. \quad (8)$$

Plugging this into the equation (2),

$$g_{1D} = \frac{1}{\hbar\pi} \sqrt{\frac{2m}{E}}. \quad (9)$$

In the case of defining the density of states for 3D, we get

$$g_{3D} = \frac{1}{V} \frac{dN}{dE}. \quad (10)$$

Following a similar derivation using the k-space as in the equation of the 1D case, we derive another equation.

$$g_{3D} = \frac{1}{2\pi^2} \left( \frac{2m}{\hbar^2} \right)^2 \sqrt{E}. \quad (11)$$

For the 1D case, we know that the energy density tends to become sparser as E increases. The relationship between the density and the different energy can be seen in Figure 2. We can observe how the density tends to zero as the energy increases, verifying the relationship of  $g_{3D} \propto \frac{1}{\sqrt{E}}$ . This is opposite to their relationship in 3D states, which is  $g_{3D} \propto \sqrt{E}$ .

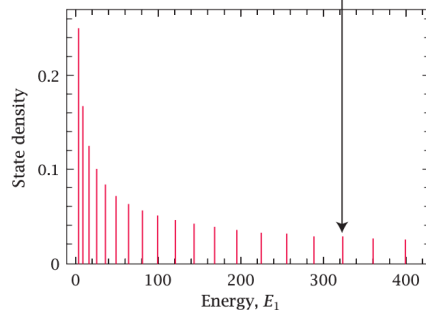


Figure 2: Density vs. Energy for 1D situation (Kuno, 2012).

## 2.2 Conductance in Metal Wires

Three regimes of conductance are present in a metal wire depending on its radius. The Drude Model, the Ballistic Transport, and Quantized Conductance.

The Drude Model assumes that the electrical transport in metals can be explained in terms of the motion of electrons. These are considered as free particles interacting with ions, at which point they collide so their valence electrons become detached and scatter in the direction of the electric field E (Ashcroft & Mermin, 1976). The model states the random occurrence of these collisions at scattering time  $\tau$  with drift velocity  $v_d$ . The semi-classical model also allows for relating the electrical conductivity or resistivity of the metal with the two mentioned variables plus the mean free time between two successful ion-ion scattering events (Trinity College Dublin, 2023).

The Ballistic Transport method tends to take place in extremely thin wires, or quasi-one-dimensional structures, where photons travel over a relatively long distance without scattering until reaching the boundary (Chen & Liu, 2022).

This has implications relating to the properties of the material, as the resistance and conductance only depend on the length of the wire (Trinity College, 2023). This has numerous applications, as it can be studied in ballistic heat conduction in, for example, graphene, where heat can be conducted without scattering (Chen & Liu, 2022).

The final regime of conductance is that of Quantized Conductance, which is the one central to our investigation. As previously mentioned, this occurs when in a one-dimensional conductor there are finite values of conductance that correspond to the number of channels that are transmitting electrons (Kittel, 2005). This concept will be prolonged in the following sections.

### 2.3 Quantum Mechanical Model of a Nanowire

Nanowires, sometimes called 'Quantum Wires', are nanostructures with a diameter that ranges in the tens of nanometers (Hobson, 2013). At this scale, quantum mechanics effects are preeminent. Because these have such unique properties, they are usually used for great systems of evaluation for dimension and size with mechanical, optical, electrical, and magnetic properties (Ozge Inal, Ulya Badilli, A. Sibel Ozkan, & Fariba Mollarasouli, 2022). These properties are affected by factors such as their morphology, the diameter-dependent band gap, the carrier density of the material, etc (Hobson, 2013).

The occurrence of quantum confinement in nanowires is one of the central properties that are relevant to this lab report. This occurs when a nanocrystal, like a nanowire, has a wavelength akin to that of the electron travelling through it as a free particle. Mohammed (2007) explains that as the nanowire's dimension reaches the exciton (electron-hole pair) Bohr Radius, its energy turns discrete. This causes the band structure of the nanocrystal to be modified, which affects the density of states and changes the "level occupancy, interband transitions, density and carrier mobility". Because this results in the quantification of the energy levels, the electrons can then only occupy specific energy states (subbands). Nanowire shown in Figure 3, where  $L \gg a$ , experiences quantum confinement in planes x and y, allowing plane z to have continuous energy levels. These adjacent subbands can be observed to correspond to a value depending on quantized energy levels  $n_x^2 + n_y^2$ , where n is the minimum value possible. This can be explained by the boundary conditions of the confined particle in a potential well. If either of these values were zero, it would be implied that the wave function didn't exist and is not constant - which is not possible. It is relevant to note that as seen in the 1D density of states section, the energy levels are actually not perfectly scaled and tend to a continuous band as the energy increases to very high levels.

For the given  $k_z$ , we can show the difference between the two lowest subbands, as they follow the quantum mechanical model of a one-dimensional infinite well. Expression for the quantization of energy for a particle in a one-dimensional infinite box is given by,

$$E_n = \frac{\hbar^2 n^2}{8ma^2}, \quad (12)$$

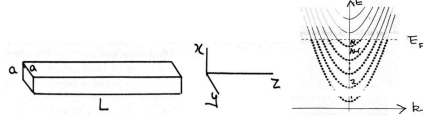


Figure 3: Geometry of nanowire and associated quantized sub-bands (Trinity College Dublin, 2023).

where we have  $n$  as the energy level  $n=1,2,3,\dots$ , and length side  $a$ . Finding the difference for  $n=1$  and  $n=2$  we get,

$$E_1 = \frac{h^2}{8ma^2}, \quad (13)$$

$$E_2 = \frac{4h^2}{8ma^2} = \frac{h^2}{2ma^2}. \quad (14)$$

Then,

$$E_2 - E_1 = \frac{h^2}{2ma^2} - \frac{h^2}{8ma^2} = \frac{3h^2}{8ma^2}. \quad (15)$$

The appropriate replacements give us the final solution,

$$E_{n_2-n_1} = \frac{3\hbar^2\pi^2}{2ma^2}. \quad (16)$$

We can use this extracted equation to find the cross-section of a side  $a < 1nm$  for an electron with mass  $m = 9.1093837E-31$  kg. Let us remember the value of the constant  $\hbar = 1.05457266E-34$  J \* s.

$$E_{spacing} = \frac{3(1.05457266 \times 10^{-34}J * s)^2\pi^2}{2(9.1093837 \times 10^{-31}kg)(1 \times 10^{-9}m)^2} \approx 1.80552 \times 10^{19} J. \quad (17)$$

We convert from J to eV,

$$E_{spacing} = \frac{1.805 \times 10^{19} J}{1.6022 \times 10^{-19}} \approx 1.127 eV. \quad (18)$$

This demonstrates that the spacing between energy levels is  $\geq 0.12$ eV. Thermal energy at temperature T is given by

$$E_{Thermal} = k_b T \quad (19)$$

with respective values  $k_b \approx 8.617 \times 10^{-5}$  eV/K and  $T = 300K$ , we get  $E_{Thermal} \approx 0.025$ . The energy spacing between the quantized subbands in the nanowire is observed to be significantly larger than the thermal energy at room temperature. This implies that at room temperature, electrons are highly unlikely to be thermally excited from one subband to another. Because they remain confined to their respective energy levels, they can be treated as existing in independent subbands.

## 2.4 Quantized Conductance

The quantized conductance observed in gold wires as they are stretched to the point of breaking provides a unique way to demonstrate quantum mechanical behaviour. This method relies on transport measurements, specifically current-voltage observations.

The experiment is done by separating two metal wires that are in contact, creating nanowires in the process. As the diameter of the gold wire diminishes to a size comparable to the de Broglie wavelength of the electrons that transport electric charge, these electron waves begin to interact with the wire's boundaries, resulting in the availability of only specific states for the electrons to traverse, as was previously mentioned.

Despite the knowledge that a normal nanostructure does not resemble an infinitely long waveguide, it was discussed how its physics of quantum transport is still surprisingly similar to that of a waveguide (Nazarov, 2009). As the electron is quantically confined and a one-dimensional system is formed, the subbands or channels are formed where only a discrete amount of current is allowed to flow. This value is proportional to the number of available conducting channels and the voltage. Considering a cube in the k-space of a nanostructure, the fraction of states filled in this cube can be called an electron filling factor,  $f(k)$ . When the wires connect and disconnect open channels occur when the subband is "open" for electron conduction. In these cases, the filling factor has two different momentum directions, as many electrons as possible will travel from the left reservoir to the right reservoir as seen in Figure 4. The filling factors depend only on the energy and the chemical potential of the corresponding reservoir. Electrons enter the nanowire from the left reservoir, which is at a higher electrochemical potential, and move toward the right reservoir, which is at a lower potential. If the Fermi energy (electrochemical potential) of the left reservoir aligns with an open channel in the nanowire, electrons can fill that channel. The filling factor then determines how many of the quantum states in that channel are occupied (Nazarov, 2009).

The explanation detailing reservoirs presented here may go beyond the scope of this laboratory, so it can be understood the way that when voltage is applied, electrons are moving from Contact 1 to Contact 2, each at different Fermi levels with the ladder having a greater one than the former. Because only the electrons moving towards Contact 2 are considered, only half of these contribute to the flow. As mentioned, Contact 2 has its own Fermi level which signifies that only the electrons with a greater level than this one can be accepted. If  $n$  is to be the number of states per unit length that Contact 2 can take electrons for the flow, we can define it with the following formula:

$$dn = \frac{g_{1D}(E_f)}{2} e \cdot dV. \quad (20)$$

Here, each infinitesimal increase of applied voltage is  $dV$  and  $dn$  is the number of additional charge carriers (Trinity College Dublin, 2023).

We now find it instructive to derive the equation for the quantum of con-

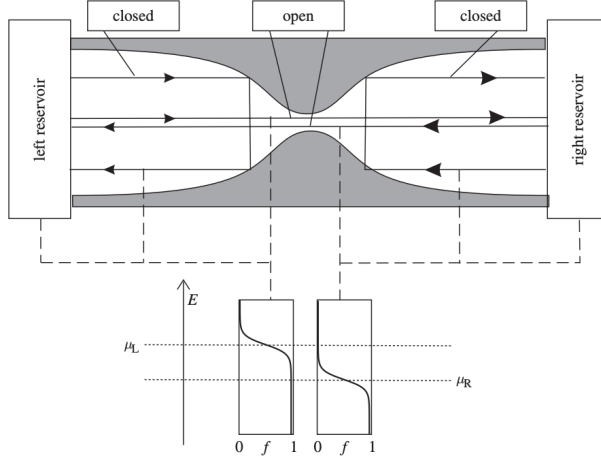


Figure 4: Filling factors in a quantum point contact for open and closed channels (Nazarov, 2009).

ductance. We have the infinitesimal relationship of electrons at the Fermi level,

$$dI = ev_f dn \quad (21)$$

with energy

$$E_f = \frac{1}{2}mv_f^2 \quad (22)$$

and velocity

$$v_f = \sqrt{\frac{2E_f}{m}}. \quad (23)$$

Replacing for  $dn$ ,

$$dI = e^2 v_f \frac{g_{1D}(E_f)}{2} \cdot dV. \quad (24)$$

Conductance  $G$  is defined as

$$G = \frac{dI}{dV}. \quad (25)$$

We replace to find,

$$G_O = \frac{e^2 v_f \frac{g_{1D}(E_f)}{2} \cdot dV}{dV} = \frac{e^2 v_f g_{1D}(E_f)}{2}. \quad (26)$$

From the section on the Density of States, we got the equation for 1D structure,

$$g_{1D} = \frac{1}{\hbar\pi} \sqrt{\frac{2m}{E}}. \quad (27)$$

For a Fermi level, we apply it to get

$$g_{1D}(E_f) = \frac{1}{\hbar\pi} \sqrt{\frac{2m}{E_f}} = \frac{1}{\hbar\pi} \sqrt{\frac{2m}{\frac{1}{2}mv_f^2}} = \frac{2}{\hbar v_f \pi}. \quad (28)$$

Plugging into the conductance,

$$G_O = \frac{e^2 v_f (\frac{2}{\hbar v_f \pi})}{2} = \frac{e^2}{\hbar\pi} = \frac{2e^2}{h}. \quad (29)$$

Our final result is then the conductance  $G_O$  with the N subbands,

$$G_O = \frac{2e^2}{h} \quad (30)$$

$$NG_0 = N \frac{2e^2}{h}. \quad (31)$$

### 3 Experimental Method

#### 3.1 Analysing Simulated Data

This part of the experiment aimed to study the phenomena and quantized conductance through the analysis of ideal and non-ideal simulated data. A Gaussian analysis is then executed on the corresponding data.

The simulated data of a voltage transient for ideal quantized conductance was drawn from the ‘SimulateQuantizedConductance.py’ pre-installed program. For this ideal transient, a number of 2500 points were selected to be produced by the storage oscilloscope. The noise amplitude was set to zero, along with the uniformity. This uniformity ensures that the randomly produced quantum conductance has quantum step changes with its exact multiples. The program was also commanded to simulate only quantized conductance changes and exclude larger, macroscopic changes. After the generated data on voltage levels and frequency counts is obtained, the voltage difference is calculated by using the formula  $\text{Col}(B)[i] - \text{Col}(B)[i+n]$ , where  $\text{Col}(B)$  is the voltage levels column. In this idealised case,  $n = 1$ . The bin centre is also chosen to be 0.08.

The non-ideal simulation is then run next. In this case, the points chosen are 250000. Because now noise is a factor to take into consideration, a more extensive range of data points is needed. Values were chosen accordingly to include noise and non-uniformity in the simulation. When calculating the voltage difference column, the value of  $n = 1$  is not appropriate anymore. Instead, we have to choose a greater value that is able to reflect the actual conductance rather than the noise. This value also can’t be too big as we might skip on valuable data. The bin values are also altered accordingly, requiring a more limiting range to get more concise data. The simulation was repeated for non-ideal conditions without noise but with non-uniform steps included.

The last section of the simulated data consisted of performing the Gaussian Least-Squared Fitting Procedure on the programme ‘TestHistogramDistributionToUse.dat’. Here we have the bin centres for the conductance difference values in the x-column and in the y-column the frequency count of the conductance differences. The first section of the analysis consisted of background subtraction. The dataset was initially “cut” by selecting data points away from the central bumps and fitting an exponential decay function to represent the background. This exponential function was subtracted from the original data, leaving a signal representing the quantized conductance changes. Next, we fit the Gaussian peaks. The residual dataset, containing the isolated signal, was fitted with a series of Gaussian peaks using Origin’s Non-Linear Curve Fit function. Four peaks were hypothesized, corresponding to integer multiples of quantized conductance. Initial estimates for the peak centres and amplitudes were provided, and through several iterations, the parameters were refined to accurately locate the positions of the conductance step changes.

### 3.2 Acquiring and Analysing Experimental Data

This section aims to experimentally demonstrate whether step changes due to quantized conductance can be recorded through nanowires in the respective setup.

To perform the experiment, we set up the oscilloscope, the amplifier and the power source (Figure 5, 6, 7). The first step was to observe the instances where the relay switches on and off. This was done by opening and closing the relay and annotating the instances in which a ‘click’ sound was produced. The instances were documented to happen at  $13.53 \pm 0.1$  V and  $14.42 \pm 0.1$  V when increasing, and at  $7.28 \pm 0.1$  V when we decreased. The oscilloscope (Figure 7) was adjusted accordingly to display the voltage signal off Channel 1. The time scale was set to  $200\mu s$  and the scale to 2.00 V. On the Channel 1 menu, the attenuation is set to ‘1X’. The number of points was set to ‘2000’. To capture the change in voltage transient, we press the ‘Run’ button and activate the trigger press by then pressing the ‘Single’ below it. The course knob is used in the power supply from minimum to maximum to capture the voltage. The trigger level is adjusted to -3.52 V accordingly.

After obtaining each frozen voltage transient graph, we need to evaluate whether this is a valuable dataset. A general indication that the phenomena of quantized conductance is present can be seen through a staircase pattern. The relay generally produces noisy signals with a hard-to-distinguish staircase pattern. In these cases, the data set is ignored and the capture process is repeated until several valuable information sets can be obtained.

To extract the data points, the ‘Tektronix’ programme on the computer needs to be opened and connected to the oscilloscope. After capturing each dataset, we copy the extracted points and pass them to OriginLab.

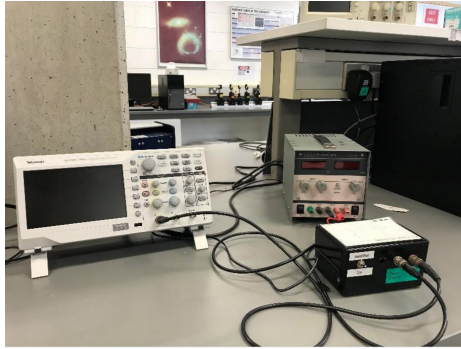


Figure 5: Experimental setup, oscilloscope, amplifier, and power source.

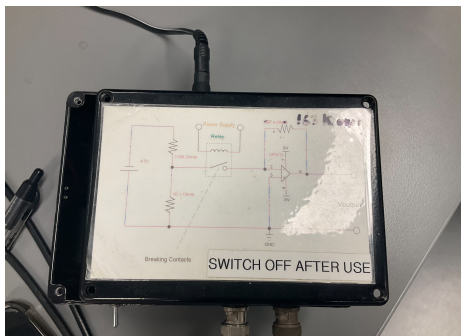


Figure 6: Power source with relay

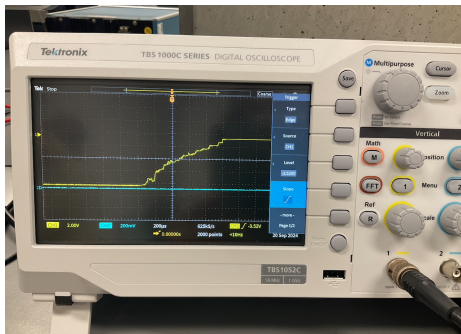


Figure 7: Oscilloscope and data sample example

## 4 Results and Discussion

### 4.1 Simulated Data

For the ideal transient, we obtain the graph of voltage cycles in Figure 8. As it was expected, it follows the staircase patterns with voltage changes that have

distinct and shape steps, which indicates the occurrence of quantized conductance. As it was explained in the Theory section, the changes in voltage levels indicated by the step changes represent a multiple of a fixed value of the conductance. It is also clear the lack of noisy data and irregularities, as there are no unexpected peaks or jumps that interrupt the uniformity of the step sizes.

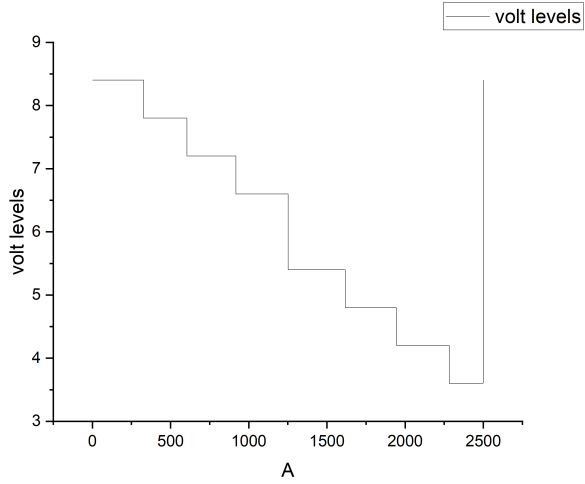


Figure 8: Graph of Ideal Voltage Steps between 0 – 8.4 V

The histogram in Figure 9 was built using a line graph as instructed, using the ‘bin centre’ on the x-axis and the ‘count’ on the y-axis after finding the voltage difference with  $n = 1$ . In the ideal scenario, we have a defined peak centred at zero that indicates the regularity of the jump pattern between the channels. We can also observe that even in an ideal simulation, the pattern is not a hundred per cent symmetrical and perfect. This could be due to the natural limitations of the system, arbitrary vertical and time scales could result in not modelling the system immaculately.

For the non-ideal noisy simulation, we obtained a graph of the voltage cycle from 3-5 V (Figure 10). Here, a value of  $n = 2$  was chosen, which results in not great data analysis as it’s too small. For future opportunities, this value has to be rectified and analyzed more profoundly.

It is abundantly clear how it changes from the one in the ideal scenario. Noise is much more prominent, causing peaks and interruptions in the smoothness of the staircase pattern. The sought-for trend is still very noticeable but with fewer perfectly sharp steps, fewer abrupt transitions, and clear fluctuations. While the shape is preserved, the deviations in the voltage levels are minor.

We also proceeded to graph the histogram for the noisy non-ideal simulation (Figure 11). We can see how the voltage differences are broader and show more of a distribution in values, not falling into direct multiples of the conductance.

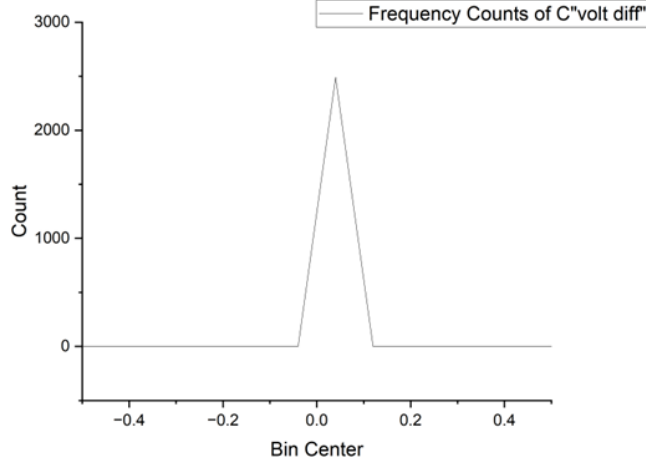


Figure 9: Histogram for ideal data, Bin Center vs. Count

The noise is the cause of the distribution.

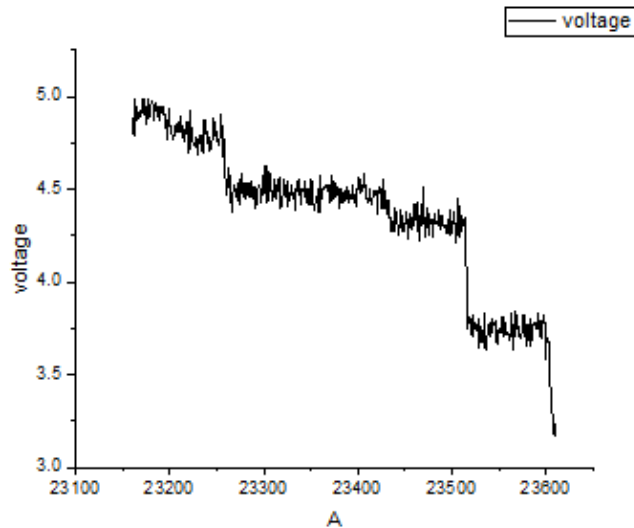


Figure 10: Graph of Ideal Voltage Steps between 3 - 5 V

Now we examine the case of the non-ideal simulation with non-uniformity and no noise. While the staircase pattern shape remains, the heights between them vary in value. This fluctuation indicates that the conductance changes are not multiples of a fixed quantum state. We can also observe that without noise,

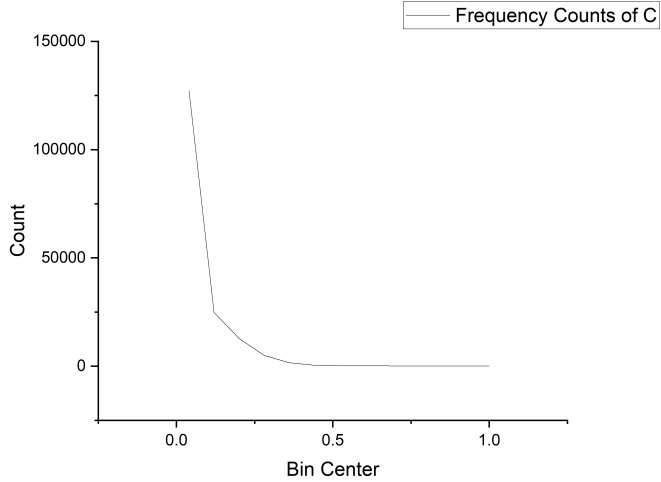


Figure 11: Histogram for non-ideal data, Bin Center vs. Count

the step sizes remain sharp. It can be clearly seen that they are much smoother than in the previous case but with higher functions between the step changes.

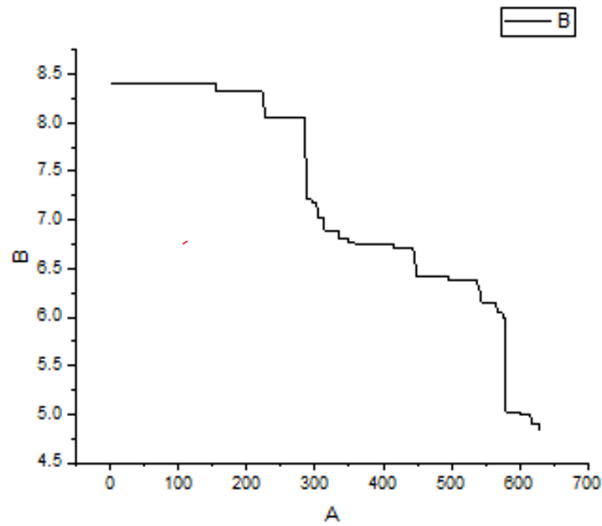


Figure 12: Graph of Voltage Steps, no noise and non-uniform simulation

The histogram peaks are no longer focused on exact multiples of the conductance quantum. The step heights are distributed, resulting in a more diffused

histogram pattern. You may see peaks that are broader and more irregularly spaced, as the step sizes are not uniform. Broader and more irregularly spaced peaks may be observed due to non-uniform step sizes.

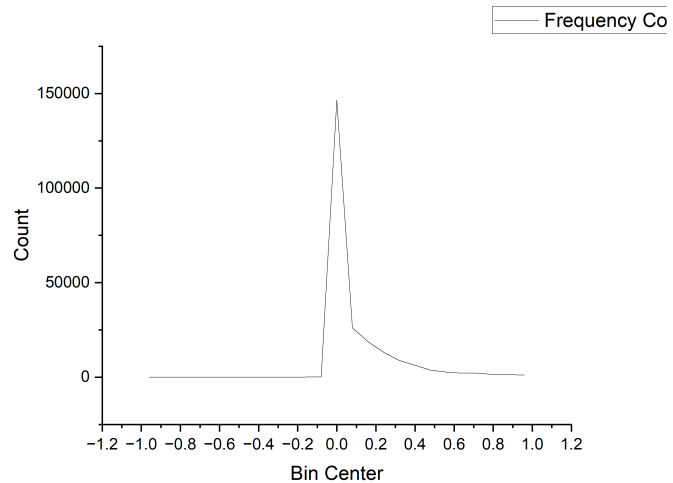


Figure 13: Histogram for No Noise Non-Uniform

## 4.2 Gaussian Fitting on Simulation

The final section of the simulation consisted of performing the Gaussian Least-Squared Fitting Procedure on the provided data set. We subtracted the data from 0.3 - 3.0, fitting the exponential function to the data outside the region of interest to isolate and eliminate background noise after the voltage differences were histogrammed. We can see in Figure 15 that there are clear imperfections in the subtraction of the data, as we do not achieve the straight, singular bump that the manual was indicating. Regardless of the attempts to increase the data points extracted from the background, this remained the same.

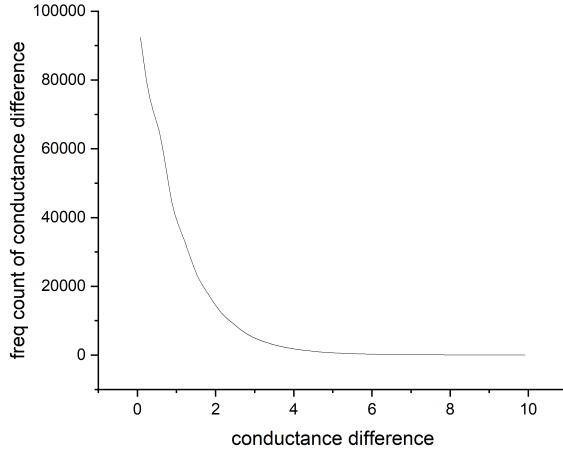


Figure 14: Gaussian Procedure Fitting on Simulated Data

Regardless, the data fitting seems to work out in Figure 16, displaying a clear pattern that aligns with what we were looking for. In this plot we can observe the distinct peaks corresponding to integer multiples of the conductance, aligning with the theory of having decreasing peaks as the multiples of the quantum conductance difference increases. While it still demonstrates some imperfections in the locations of the peaks, the overall trend remains relevant. The peaks were approximately equally spaced. The spacing between peaks was found to be around 0.6 quantum units, representing the transition between discrete conductance channels. The measured distances between peaks were: Peak 1 to Peak 2:  $0.6044 \pm 0.0043$ , Peak 2 to Peak 3:  $0.5491 \pm 0.0102$ , and Peak 3 to Peak 4:  $0.5591 \pm 0.0229$ . For the conductance, the following equation was used:

$$\Delta G_O = \frac{-\Delta V_{out}}{R_2 V_{in}} \quad (32)$$

with respective values  $R_2 = 163k\Omega$  and  $V_{in} = 4.5V$ .

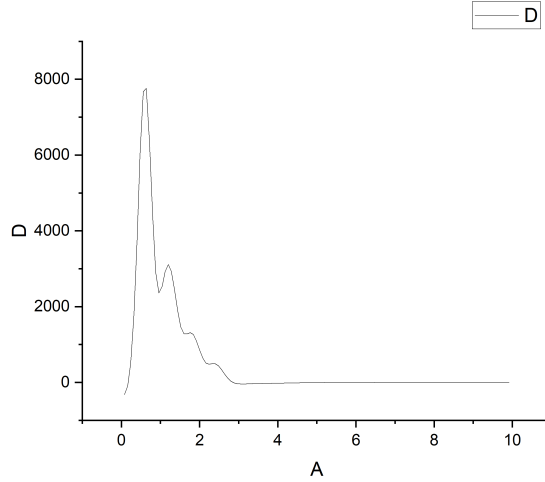


Figure 15: Gaussian Procedure Fitting on Simulated Data

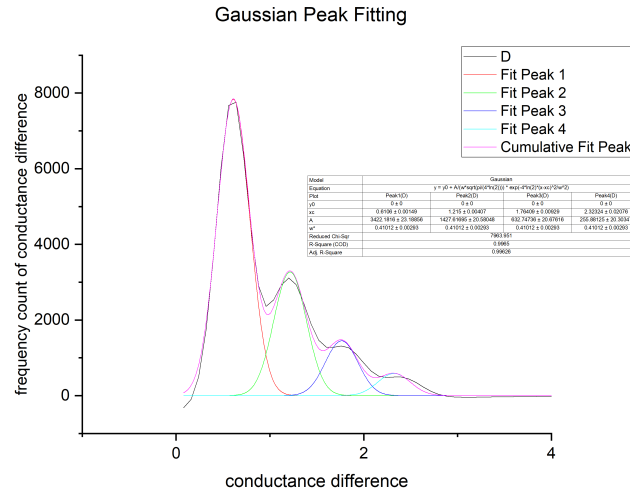


Figure 16: Gaussian Procedure Fitting on Simulated Data

### 4.3 Experimental Data

Figures 17 and 18 show specific data extraction samples from the experimental data. From these, we can see clearly the staircase pattern's general trend, although it defers greatly from the ideal simulation. We can see the role of both noise and non-uniformity in the data. For example, in both cases, the step sizes

are not smooth but suffer from peak intrusions between each level. They also lack clear differences between levels, as we see that one step seems to blend with the next. All of this can be attributed to the highly flawed ordeal of measuring such specific and delicate phenomena as quantum conductance. Noise, thermal fluctuations, and potential atomic-scale structural variations can be attributed to this more erratic pattern.

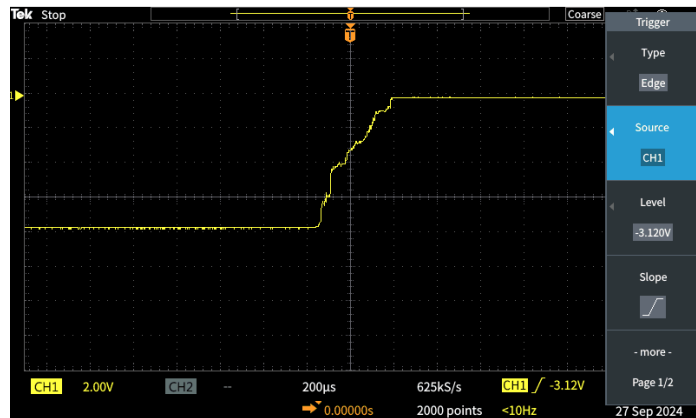


Figure 17: Data Extraction Example

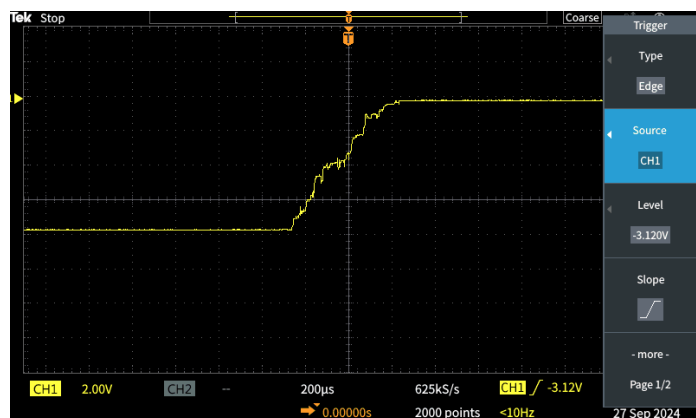


Figure 18: Data Extraction Example

As in the ideal scenario, the voltage differences histogram from the experimental data did not display distinct, sharp peaks. Rather, it was more challenging to discern distinct quantized steps in the conductance due to the peaks' broader appearance. Figure 19 shows the histogram extracted from the data, which does not assimilate the patterns we got for the simulations or the ones we would expect. Despite attempting to cut the background noise and unaccounted impurities, the yielding Gaussian fit shown in Figure 20 does not display distinct values for the multiples of the representing conductance that we got for the simulation. This is regardless to be expected, as such quantum occurrence is very sensitive and hard to measure in scales such as those of the nanowire. From the gathered information of the plot, we get  $G_0 \approx 6.4 \times 10^{-7}$ , which is two orders of magnitude off the actual value  $G_0 = 7.748 \times 10^{-5}$ .

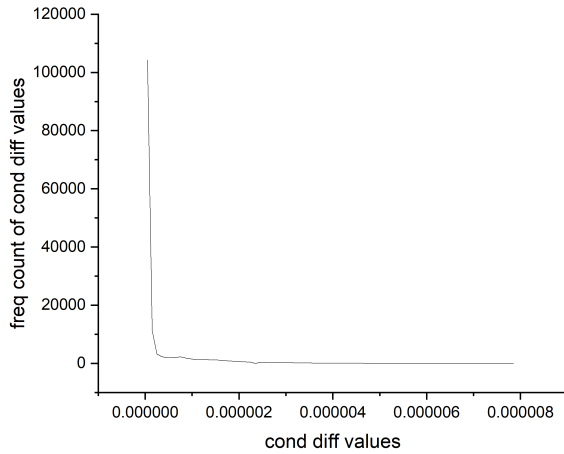


Figure 19: Histogram of Experimental Data

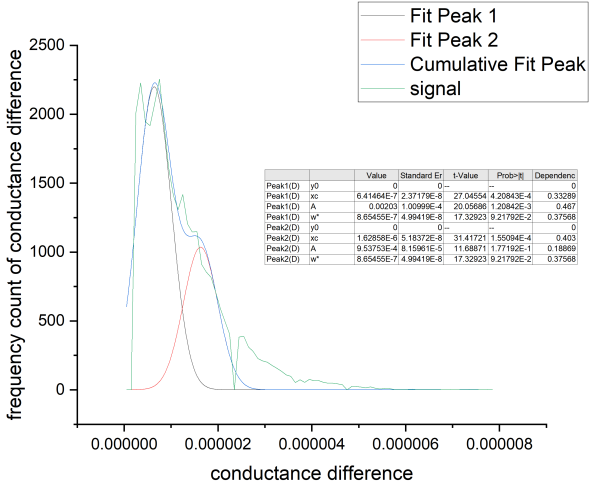


Figure 20: Gaussian Fit of Experimental Data

## 5 Conclusion

We can conclude that the results reveal both the potential and challenges associated with quantifying conductance in nanowires. While the staircase pattern was always visible with varying degrees of clarity, the exhibition of significant noise and non-uniformity was a source of complication for the experimental analysis. The differences between the measured values and theoretical predictions highlight the sensitivity of quantum conductance measurements to environmental factors. The Gaussian Fit seemed to work well for the simulation, but the extraction of background data did not yield much success for the actual experimental result. Future research should focus on optimizing measurement techniques and minimizing extraneous noise to improve data accuracy. Despite the limitations, this investigative work was able to explore the phenomena of quantized conductance while exhibiting room for improvement when studying nanostructures and quantum behaviour.

## 6 References

- Ashcroft, N. W., & Mermin, N. D. (1976). Solid state physics. Holt, Rinehart and Winston.
- Chen, J., & Liu, B. (2022). Ballistic heat conduction characteristics of graphene nanoribbons. *Physica E Low-Dimensional Systems and Nanostructures*, 139, 115146–115146.
- Hobson, D. W. (2011). Nanotechnology. Elsevier EBooks, 683–697.
- King, D. (2005). Density of states: 2D, 1D, and 0D. Georgia Institute of Technology.
- Kittel, C. (2005). Introduction to solid state physics (8th ed.). Wiley.
- Kuno, M. (2012). Introductory nanoscience: Physical and chemical concepts (1st ed.). Wiley.
- Mohammad, S. (2014). Understanding quantum confinement in nanowires: Basics, applications and possible laws. *Journal of Physics: Condensed Matter*.
- Nazarov, Y. V., & Blanter, Y. M. (2009). Quantum Transport: Introduction to Nanoscience. Cambridge: Cambridge University Press.
- Ozge Inal, Ulya Badilli, A. Sibel Ozkan, & Fariba Mollarasouli. (2022). Bioactive hybrid nanowires for drug delivery. Elsevier EBooks, 269–301.
- Trinity College Dublin. (2023). Junior Sophister Laboratory: Quantized conductance. Department of Physics, Trinity College Dublin.